A passive method to compensate nonlinearity in a homodyne interferometer

Jeongho Ahn,[1] Jong-Ahn Kim,[2] Chu-Shik Kang,[2] Jae Wan Kim,[2*] and Soohyun Kim[1,]

[1]*Division of Mechanical Engineering, KAIST, 335 Gwahangno, Yuseong-gu, Daejeon, 305-701, Republic of Korea*
[2]*Length/Time Center, KRISS, 209 Gwahangno, Yuseong-gu, Daejeon, 305-340, Republic of Korea*
**jaewan@kriss.re.kr*

Abstract: This study presents an analysis of the nonlinearity resulting from polarization crosstalk at a polarizing beam splitter (PBS) and a wave plate (WP) in a homodyne interferometer. From a theoretical approach, a new compensation method involving a realignment of the axes of WPs to some specific angles according to the characteristics of the PBS is introduced. This method suppresses the nonlinearity in a homodyne interferometer to 0.36 nm, which would be 3.75 nm with conventional alignment methods of WPs.

OCIS codes: (120.0120) Instrumentation, measurement, and metrology; (120.3180) Interferometry.

References and links

1. I. Misumi, S. Gonda, T. Kurosawa, and K. Takamasu, "Uncertainty in pitch measurements of one-dimensional grating standards using a nanometrological atomic force microscope," Meas. Sci. Technol. **14**(4), 463–471 (2003).
2. P. L. M. Heydemann, "Determination and correction of quadrature fringe measurement errors in interferometers," Appl. Opt. **20**(19), 3382–3384 (1981).
3. C.-M. Wu, C.-S. Su, and G.-S. Peng, "Correction of nonlinearity in one-frequency optical interferometry," Meas. Sci. Technol. **7**(4), 520–524 (1996).
4. T. B. Eom, J. Y. Kim, and K. Jeong, "The dynamic compensation of nonlinearity in a homodyne laser interferometer," Meas. Sci. Technol. **12**(10), 1734–1738 (2001).
5. J.-A. Kim, J. W. Kim, C.-S. Kang, T. B. Eom and J. Ahn, "A digital signal processing module for real-time compensation of nonlinearity in a homodyne interferometer using a field-programmable gate array," Meas. Sci. Technol 20(1), 017003.1–017003.5 (2009).
6. T. Keem, S. Gonda, I. Misumi, Q. Huang, and T. Kurosawa, "Simple, real-time method for removing the cyclic error of a homodyne interferometer with a quadrature detector system," Appl. Opt. **44**(17), 3492–3498 (2005).
7. Z. Li, K. Herrmann, and F. Pohlenz, "A neural network approach to correcting nonlinearity in optical interferometers," Meas. Sci. Technol. **14**(3), 376–381 (2003).
8. O. P. Lay, and S. Dubovitsky, "Polarization compensation: a passive approach to a reducing heterodyne interferometer nonlinearity," Opt. Lett. **27**(10), 797–799 (2002).
9. G. Dai F. Pohlenz, H.-U. Danzebrink, K. Hasche, and G. Wilkening, "Improving the erformance of interferometers in metrological scanning probe microscopes," Meas. Sci. Technol. **15**(2), 444–450 (2004).

1. Introduction

Nonlinear error of homodyne laser interferometers is principally caused by imperfection of optics used in an interferometer. In fact, nonlinear error in an interferometer represents the practical limit of its measuring capability when measuring in a small target region of less than several tens of micrometers [1–5].

Several compensation methods to reduce the nonlinearity in the displacement measurements of interferometers have been suggested. The first method, by Heydemann [2], was followed by the dynamic compensation method [4,5], the gain adjustment method [6], and the neural network approach [7]. All of these approaches have shown a good capability to reduce the nonlinearity. However, all of these methods also have their limits for many reasons. In case of [2–4] and [7], they use elliptical fitting method which requires reliable abundant data and time for processing. Therefore, they cannot be applied to such a system as

#119009 - $15.00 USD Received 23 Oct 2009; revised 19 Nov 2009; accepted 19 Nov 2009; published 4 Dec 2009

demands the real-time compensation. The gain adjustment method [6] is very simple so that it can be a candidate for fast compensating method. However, it can compensate only the difference of amplitude and offset between the final two sinusoidal signals. The phase delay, or lack of quadrature still remains as the nonlinearity source.

The new compensation method introduced in this paper differs in that it adopts a passive compensation method. A passive compensation method was once introduced earlier [8], but it was for a heterodyne interferometer and could not sufficiently explain overall optical crosstalk analytically and numerically. It only mentioned about linear polarization and its removal method by rotating linear polarizer. However, practically there exist elliptically polarized beam in the optical crosstalk due to the phase retardation passing through optical elements.

A general homodyne interferometer with a quadrature detection system [6] was adopted for this research, and its optical configuration is shown in Fig. 1. There are three quarter-wave plates (QWPs) and one half-wave plate (HWP), and their alignment axes can be adjusted on rotation mounts. The key idea of the proposed passive compensation method is to realign the axes of wave plates (WPs) to specific angles that are dependent on the characteristics of a polarizing beam splitter (PBS) to minimize nonlinear error. The passive compensation method can suppress the innate nonlinearity of an interferometer and is able to cooperate with a simple active compensation method, such as gain and offset correction [9], to remove nonlinearity more effectively.

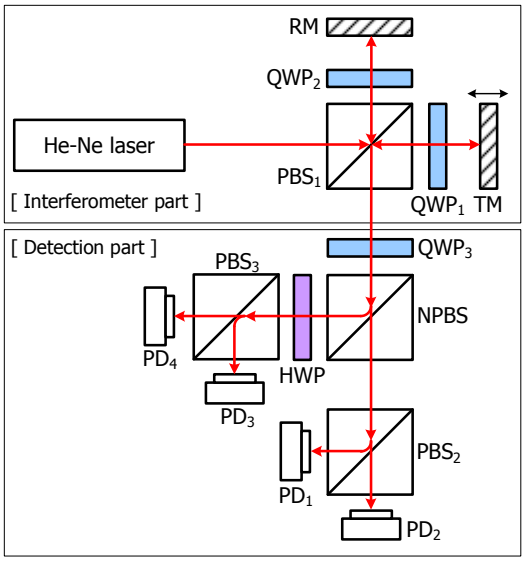

Fig. 1. Simple diagram of a homodyne interferometer with quadrature detection system: Polarizing Beam Splitter (PBS), Quarter-Wave Plate (QWP), Reference Mirror (RM), Target Mirror (TM), Non-Polarizing Beam Splitter (NPBS), Half-Wave Plate (HWP), Photo Diode (PD)

2. Nonlinearity in the homodyne interferometer

In the ideal case, the intensity signals at the end of interferometer with quadrature detection system should be two sinusoids, which have a 90° phase difference from each other and same amplitude as shown in Eq. (1). Therefore, the phase θ can be acquired by using the simple Eq. (2).

$$I_x = A\cos\theta \quad , \quad I_y = A\sin\theta \tag{1}$$

$$\theta = \arctan(I_y / I_x) \tag{2}$$

#119009 - $15.00 USD Received 23 Oct 2009; revised 19 Nov 2009; accepted 19 Nov 2009; published 4 Dec 2009

On the contrary, in the real case they have not only different amplitude and offset but also lack of quadrature, δ as in Eq. (3) [3]. This might be caused by the gain difference of photo detector or electrical noise. However, the main reason is phase mixing caused by the imperfection of optical elements such as PBS, QWP and HWP.

$$I_x = A\cos\theta + B \quad , \quad I_y = C\sin(\theta + \delta) + D \tag{3}$$

Using Eq. (2) to calculate the phase from Eq. (3) induces nonlinearity. To get the exact phase from the signals in Eq. (3), an elliptical fitting method is usually applied. Then, except for the effects from electrical noise, short-term power instability of light source, and numerical fitting error, the obtained phase is free from the nonlinearity. However, as mentioned in section 1, elliptical fitting is a time-consuming process so that it cannot be used for the real-time compensating method. A new compensation method that is fast and highly capable of nonlinearity suppression will be introduced in the next section.

3. Passive compensation method

3.1 Principle of the passive compensating method

Due to the polarization crosstalk, the quadrature signals from the photo diodes are expressed as in Eq. (3). A simple nonlinearity compensation method is to correct the gain and offset in the Eq. (3). It is not a time-consuming process like elliptical fitting, so that it can be applied to the real-time compensation. Obtaining the parameters, A, B, C and D from one period of sinusoidal signal is easy using simple arithmetical operation [9].

After these four parameters are obtained, $I_x^{'}$ and $I_y^{'}$ can be determined as in Eq. (4). They have unit amplitude and no offset, except the lack of quadrature, δ.

$$\begin{aligned} I_x^{'} &= (I_x - B)/A = \cos\theta \\ I_y^{'} &= (I_y - D)/C = \sin(\theta + \delta) \end{aligned} \tag{4}$$

Applying Eq. (2) with $I_x^{'}$ and $I_y^{'}$ gives a good compensation result, even though the effect of lack of quadrature, δ still remains. However, as the phase error δ becomes larger, the compensating capability gets weaker. The lack of quadrature δ can be roughly converted into the displacement error as in Eq. (5) for the single pass interferometer.

$$\Delta x \approx \frac{\lambda \cdot \delta}{4\pi} \tag{5}$$

In the case of a He-Ne laser (λ = 632.8 nm), 1.14° of lack of quadrature induces 1 nm of nonlinearity, therefore, the phase error δ should also be compensated for the sub-nanometer accuracy.

Figure 2(a) shows an optical element which induces polarization crosstalk so that the transmitted light has phase retardation. However, if a WP can compensate the phase retardation, the orthogonally polarized electric fields of emitting light will be in phase (Fig. 2 (b)). By this principle, adjusting the rotation angles of a WP in the interferometer can compensate for the lack of quadrature δ. This is the basic principle of the passive compensation of the nonlinearity in the interferometer. Actually, describing the phase mixing and the compensation by WP alignment in the interferometer is more complicated, however, the basic principle mentioned above is representing the compensation so clearly that no additional equation is necessary.

#119009 - $15.00 USD Received 23 Oct 2009; revised 19 Nov 2009; accepted 19 Nov 2009; published 4 Dec 2009

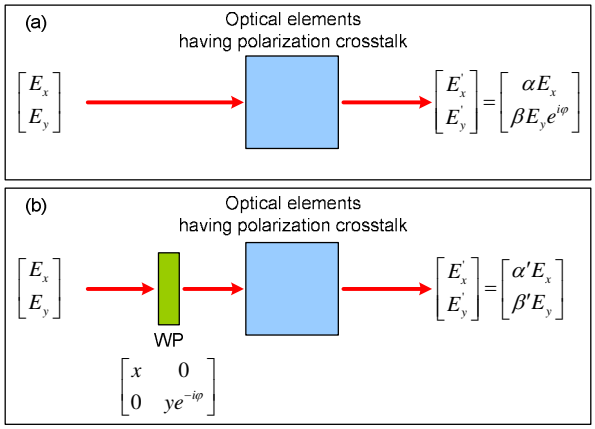

Fig. 2. The principle of passive compensation method

3.2 Jones matrix of optical elements

For optical model of interferometer the Jones matrix and Jones vector will be used. To describe the real optical elements some modified Jones matrices is introduced in this section.

The Jones matrix for an ideal PBS has only diagonal elements. On the other hand, the Jones matrix for a real PBS requires modification, as described by Eq. (6), to describe the real beam-splitting phenomenon.

$$\mathbf{T} = \begin{bmatrix} t_p & t_s^c \\ t_p^c & t_s \end{bmatrix} \qquad \mathbf{R} = \begin{bmatrix} r_p & r_s^c \\ r_p^c & r_s \end{bmatrix} \tag{6}$$

T and **R** in Eq. (6) are the transmission and the reflection matrices, respectively. The values t and r denote the transmissivity and reflectivity, and the subscripts p and s represent the polarization state. Finally, the superscript c represents the optical crosstalk.

These characteristic matrices can be roughly determined through a simple experiment using high extinction ratio polarizers, a polarizing beam splitter and photo detectors as in Fig. 3. This experiment to characterize the PBS should be performed prior to the setup of the interferometer. The HWP is for rotating the axis of linear polarization so that a vertically polarized (s-polarized) or horizontally polarized (p-polarized) beam can be produced. A polarizer, P1 which has high extinction ratio about 10000:1, is placed after the HWP so that the transmitted light is mostly polarized linearly, and after the PBS, the same kind of polarizers, P2 and P3 are placed just before the photo detector PD1 and PD2.

The procedure is as follows: First, rotate the HWP to make a p-polarized beam, and make the transmission axis of P1 to coincide with the axis of the linearly polarized beam. This allows most of the beam to transmit the PBS with a high extinction ratio. After the PBS, by rotating the P2 or P3, the intensity of the s- and p-polarized beam can be measured. For the s-polarized beam the same experiment is conducted to get the intensities of each polarization state. Through the measured intensity, the parameters of the Jones matrix can be determined, and this procedure is expressed through Eqs. (7) to (12).

$$\begin{bmatrix} E_x^t \\ E_y^t \end{bmatrix} = \begin{bmatrix} t_p & t_s^c \\ t_p^c & t_s \end{bmatrix} \begin{bmatrix} E_x \\ E_y \end{bmatrix} \tag{7}$$

$$\begin{bmatrix} E_x^r \\ E_y^r \end{bmatrix} = \begin{bmatrix} r_p & r_s^c \\ r_p^c & r_s \end{bmatrix} \begin{bmatrix} E_x \\ E_y \end{bmatrix} \tag{8}$$

#119009 - $15.00 USD Received 23 Oct 2009; revised 19 Nov 2009; accepted 19 Nov 2009; published 4 Dec 2009

Equations (7) and (8) describe the electric fields at the points 'a', 'b' and 'c' shown in Fig. 3, and their relation. Because only intensity can be detected at the photo detector, Eqs. (7) and (8) need to be modified into intensity relations as Eqs. (9) to (12).

$$I_x^t = E_x^t \cdot E_x^{t*} = \left(t_p\right)^2 \cdot \left|E_x\right|^2 + \left(E_x \cdot E_y^* + E_y \cdot E_x^*\right) \cdot t_p t_s^c + \left(t_s^c\right)^2 \cdot \left|E_y\right|^2 \quad (9)$$

$$I_y^t = E_y^t \cdot E_y^{t*} = \left(t_p^c\right)^2 \cdot \left|E_x\right|^2 + \left(E_x \cdot E_y^* + E_y \cdot E_x^*\right) \cdot t_p^c t_s + \left(t_s\right)^2 \cdot \left|E_y\right|^2 \quad (10)$$

$$I_x^r = E_x^r \cdot E_x^{r*} = \left(r_p\right)^2 \cdot \left|E_x\right|^2 + \left(E_x \cdot E_y^* + E_y \cdot E_x^*\right) \cdot r_p r_s^c + \left(r_s^c\right)^2 \cdot \left|E_y\right|^2 \quad (11)$$

$$I_y^r = E_y^r \cdot E_y^{r*} = \left(r_p^c\right)^2 \cdot \left|E_x\right|^2 + \left(E_x \cdot E_y^* + E_y \cdot E_x^*\right) \cdot r_p^c r_s + \left(r_s\right)^2 \cdot \left|E_y\right|^2 \quad (12)$$

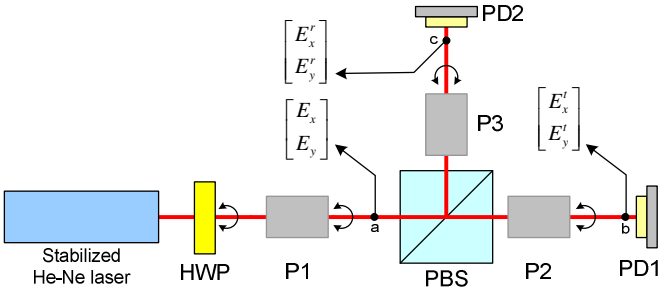

Fig. 3. Experiment setup for measuring the optical properties of PBS: Half-Wave Plate (HWP), Polarizing Beam Splitter (PBS), Polarizer (P), Photo Detector (PD)

When the incident beam is *p*-polarized at the point 'a', the amplitude of E_x is much larger than that of E_y. Therefore, the second and third terms in Eqs. (9) to (12) can be neglected, and from the simplified equation, t_p, t_p^c, r_p and r_p^c can be determined. When the incident beam is *s*-polarized beam, or the amplitude of E_y is much larger than that of E_x, the first and second term in Eqs. (9) to (12) vanish. Then, t_s^c, t_s, r_s^c and r_s are determined in the same manner. Table 1 shows how to obtain all the parameters of the Jones matrices from intensity data.

Table 1. Calculation of Jones matrix parameters that represent the transmission and reflection properties of the polarizing beam splitter

Parameters of Jones matrix	
Transmission	Reflection
$t_p = \sqrt{I_x^t / I_x}$	$r_p = \sqrt{I_x^r / I_x}$
$t_p^c = \sqrt{I_y^t / I_x}$	$r_p^c = \sqrt{I_y^r / I_x}$
$t_s^c = \sqrt{I_x^t / I_y}$	$r_s^c = \sqrt{I_x^r / I_y}$
$t_s = \sqrt{I_y^t / I_y}$	$r_s = \sqrt{I_y^r / I_y}$

It is well known that in a homodyne interferometer that uses quadrature detection, the WPs should be aligned with its fast axis at 45° for QWP and 22.5° for HWP. However, to minimize the nonlinearity caused by the optical crosstalk, the WPs should not be aligned at the conventional angles according to the suggested passive compensation method in this paper. Instead the WPs need to be aligned at the specific angle relying on the characteristic properties of the PBS. Therefore, an extended formula of the Jones matrix for WP aligned at

#119009 - $15.00 USD Received 23 Oct 2009; revised 19 Nov 2009; accepted 19 Nov 2009; published 4 Dec 2009

arbitrary angle is required to approach the new compensation method numerically. The Jones matrix, **W**, for a WP aligned at an arbitrary angle ($\psi + \Delta\theta$) can be expressed as in Eqs. (13) and (14), where $\mathbf{W_o}$ is the Jones matrix of a WP with phase retardation tolerance ε with its fast axis at 0° and **R** is a rotation matrix. The nominal value of rotation angle parameter ψ is $\pi/4$ for QWP and $\pi/8$ for HWP, and $\Delta\theta$ is the deviation angle from ψ. Γ denotes the nominal phase retardation of the wave plate, which is $\pi/2$ for the QWP and π for the HWP.

$$\mathbf{W} = \mathbf{R}(-(\psi + \Delta\theta))\mathbf{W_o}\mathbf{R}(\psi + \Delta\theta) = \begin{bmatrix} w_{11} & w_{12} \\ w_{21} & w_{22} \end{bmatrix} \tag{13}$$

$$\begin{aligned} w_{11} &= e^{-i(\Gamma/2+\varepsilon/2)}\cos^2(\psi+\Delta\theta) + e^{i(\Gamma/2+\varepsilon/2)}\sin^2(\psi+\Delta\theta) \\ w_{21} &= -i\sin(\Gamma/2+\varepsilon/2)\sin(2(\psi+\Delta\theta)) \\ w_{12} &= -i\sin(\Gamma/2+\varepsilon/2)\sin(2(\psi+\Delta\theta)) \\ w_{22} &= e^{-i(\Gamma/2+\varepsilon/2)}\sin^2(\psi+\Delta\theta) + e^{i(\Gamma/2+\varepsilon/2)}\cos^2(\psi+\Delta\theta) \end{aligned} \tag{14}$$

3.3 Optical model of single pass homodyne interferometer

In Fig. 1, the incident ray is linearly polarized at 45°. The *p*-polarized beam transmits PBS_1 and QWP_1, and then reflected from TM. As it passes through the QWP_1 twice, the *p*-polarization changes to *s*-polarization so that it is reflected at the PBS_1 and propagates to the detection part. Contrary to the *p*-polarization, the *s*-polarized beam reflects from the PBS_1 and passes through QWP_2. After reflecting from RM and passing through QWP_2 again, the *s*-polarization also changes to *p*-polarization. Therefore, it can transmit the PBS_1 and proceed for the detection part. The propagation of *s*- and *p*-polarization elements of incident beam in the interferometer part can be described using the Jones matrix as in the following equations.

$$\mathbf{E_{tar}} = \mathbf{R_1}\mathbf{Q_{\psi_1}}\mathbf{e^{i\varphi}}\mathbf{R_m}\mathbf{e^{i\varphi}}\mathbf{Q_{\psi_1}}\mathbf{T_1}\mathbf{E_{in}} \tag{16}$$

$$\mathbf{E_{ref}} = \mathbf{T_1}\mathbf{Q_{\psi_2}}\mathbf{R_m}\mathbf{Q_{\psi_2}}\mathbf{R_1}\mathbf{E_{in}} \tag{17}$$

In Eqs. (16) and (17), $\mathbf{E_{tar}}$ and $\mathbf{E_{ref}}$ are the resultant electric field passed through the target arm and the reference arm respectively. $\mathbf{Q_{\psi j}}$ is the Jones matrix for the j_{th} QWP (j = 1,2,3) that is angularly aligned at ψ_j, and $\mathbf{T_j}$ and $\mathbf{R_j}$ denote the transmission and reflection matrix of the j_{th} PBS (j = 1,2,3). In addition, $\mathbf{E_{in}}$ is the electric field vector of the incident ray, and $\mathbf{R_m}$ is a reflection matrix of a target mirror and a reference mirror. φ is the relative phase change due to the target mirror movement. At the entrance of the detection part, there are two electric fields, $\mathbf{E_{tar}}$ and $\mathbf{E_{ref}}$, which have traveled different arms of the interferometer. The sum of these two fields is to be denoted as $\mathbf{E_{int}}$. In the detection part, $\mathbf{E_{int}}$ experiences several polarization optical parts, as expressed by Eqs. (18) to (21). $\mathbf{H_\psi}$ is the Jones matrix for the HWP whose fast axis is at ψ, *T* and *R* denote the transmission and reflection coefficient of the NPBS. $\mathbf{D_j}$ represents the resultant electric field at the j_{th} photo detector (j = 1,…,4). As the intensity is proportional to $|\mathbf{D_j}|^2$, the final interferometric signals and nonlinear error can be analyzed using the aforementioned equations.

$$\mathbf{D_1} = \mathbf{R_2}T\mathbf{Q_{\psi_3}}\mathbf{E_{int}} \tag{18}$$

$$\mathbf{D_2} = \mathbf{T_2}T\mathbf{Q_{\psi_3}}\mathbf{E_{int}} \tag{19}$$

$$\mathbf{D_3} = \mathbf{R_3}\mathbf{H_\psi}R\mathbf{Q_{\psi_3}}\mathbf{E_{int}} \tag{20}$$

$$\mathbf{D_4} = \mathbf{T_3}\mathbf{H_\psi}R\mathbf{Q_{\psi_3}}\mathbf{E_{int}} \tag{21}$$

#119009 - $15.00 USD Received 23 Oct 2009; revised 19 Nov 2009; accepted 19 Nov 2009; published 4 Dec 2009

3.4 Simulation and Analysis

A simulation to determine the magnitude of the nonlinear error in measuring the displacement was performed with various angular configurations of the WPs. As shown in Fig. 1, the homodyne interferometer setup is assumed and its light source is a He-Ne laser (λ = 632.8nm) with less than 1% of intensity fluctuation. By using the method introduced in section 3.2, the transmission matrix and the reflection matrix were determined experimentally as $\mathbf{T_1}$ = [0.9413, 0.0127; 0.0203, 0.0430] and $\mathbf{R_1}$ = [0.2629, 0.0278; 0.0137, 0.9788]. Both $\mathbf{T_2}$ and $\mathbf{T_3}$ are given by [0.9777, 0.0009; 0.0133, 0.0137]; both $\mathbf{R_2}$ and $\mathbf{R_3}$ are given by [0.0405, 0.0146; 0.0115, 0.9837]. Because PBS_1 is tilted about 5° to prevent from the multi-interference by ghost reflections in the experimental setup, its property is a little different from that of PBS_2 and PBS_3. The WPs were assumed to have a phase retardation error value ε of $\pi/250$, the value of which was taken from the manufacture's specifications.

The results, shown in Fig. 4, indicate that the nonlinear error is reduced to a minimum at the specific angles other than the nominal values of 45° and 22.5°. From an observation of the curves in Fig. 4, the alignment state of the HWP is most sensitive to the nonlinearity. The rotation angle of QWP_2 shows a small variation to the nonlinearity error. Moreover, the angular alignment states of respective WPs are coupled in determining the magnitude of the nonlinear error. Therefore, a set of angular alignment values can be optimized, which minimizes the nonlinear error.

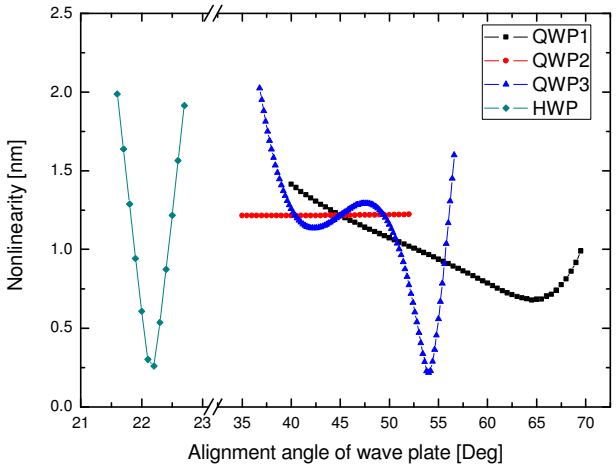

Fig. 4. Nonlinear error according to the alignment angle of wave plates: When the axis of the alignment angle of the QWP_1 rotates, the alignment axes of other WPs are fixed. The QWP_2, QWP_3, and HWP graphs are obtained in the same manner.

In Fig. 5, the solid line shows the expectation of cyclic nonlinear error caused by the imperfection of optical elements. When only the gain and offset correction method is applied with all WPs aligned at the nominal value, its peak-to-valley value is 1.216 nm, and the lack of quadrature is 1.38°. For the optimization, the nonlinear error was initially defined as a function of the WP alignment angles of the QWPs and HWP using the Matlab optimization function. The step size of the angle variation was set to 0.1°, which is the minimum resolution available from rotational mounts. Through the optimization process, the set of angles for alignment of WPs are determined as 51.3° for QWP_1, 18.9° for QWP_2, 50.5° for QWP_3, and 22.2° for HWP. By setting the WPs to these angles in the simulation, the magnitude of nonlinear error was reduced to 0.057 nm, which is much smaller than the original magnitude of nonlinear error, and the lack of quadrature is 0.022°. As expected, the passive method

#119009 - $15.00 USD Received 23 Oct 2009; revised 19 Nov 2009; accepted 19 Nov 2009; published 4 Dec 2009

effectively suppressed the lack of quadrature which still remained after applying the gain and offset correction method.

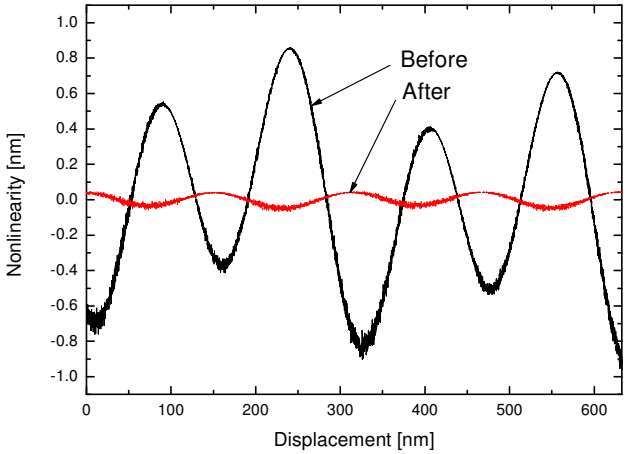

Fig. 5. Theoretically predicted nonlinear error in a homodyne interferometer: The passive compensation method suppresses the innate nonlinearity of the homodyne interferometer effectively.

4. Experiments

4.1 Setup

The system for evaluation of passive compensation method comprises an interferometer module and signal processing module. To set up the homodyne interferometer, 30 mm cage system is adopted for easy alignment and for reducing the effect from environmental vibration. In addition, to minimize the error from air turbulence, the path length of the interferometer is determined as short as possible. The WPs are set on a rotatable mount to adjust the transmission axis. Triangle wave voltage signal is generated at PC and amplified by a high voltage amplifier to operate the fine motion stage which has a range of several micrometers according to the Z axis. 0.2 Hz of triangle wave is induced to the fine motion stage and the stage moves almost a wavelength of the He-Ne laser. The LabView user interface program displays Lissajous graph and interference signals and conducts data processing to measure the nonlinearity. Basically, the gain and offset correction method is applied to the raw interference signal, and use Eq. (2) to calculate the displacement of the stage. The stage does not move linearly according to the applied voltage for the nonlinear characteristic of a piezo actuator. Therefore, fitting the calculated displacement for the applied voltage to the third polynomial is required to remove the nonlinearity of piezo actuator. The residual in the fitting process is the nonlinearity in the interferometer. The nonlinearity of piezo actuator has much lower frequency than that of interferometer, so that the fitting process could not change the original value of nonlinearity in the interferometer.

4.2 Result and discussion

When all WPs are aligned at the nominal value, the magnitude of nonlinearity is 3.75 nm in the peak-to-valley value, and the lack of quadrature is 4.74°. The same procedure aforementioned in section 3.4 is used for an experiment to measure the nonlinearity at the various alignment conditions of WPs. Figure 6(a) to 6(d) shows the experimental result of the

#119009 - $15.00 USD Received 23 Oct 2009; revised 19 Nov 2009; accepted 19 Nov 2009; published 4 Dec 2009

each WP comparing with the theoretically expected value. There are some difference between the theoretical expectation and experimental result in the magnitude and the alignment angle showing the minimum nonlinearity. The exact characteristic parameters are necessary to approach the nonlinearity theoretically, but this is not available in practice. For this reason, the experimental results show little differences compared to the theoretical expectation. However, both of them are representing similar tendency: HWP is most sensitive in determining the nonlinearity, and the curve for QWP_3 has two minimum points. The angle with minimum nonlinearity for QWP_1 coincides in the theoretical expectation and experimental result, and the curve for QWP_2 is almost flat as predicted.

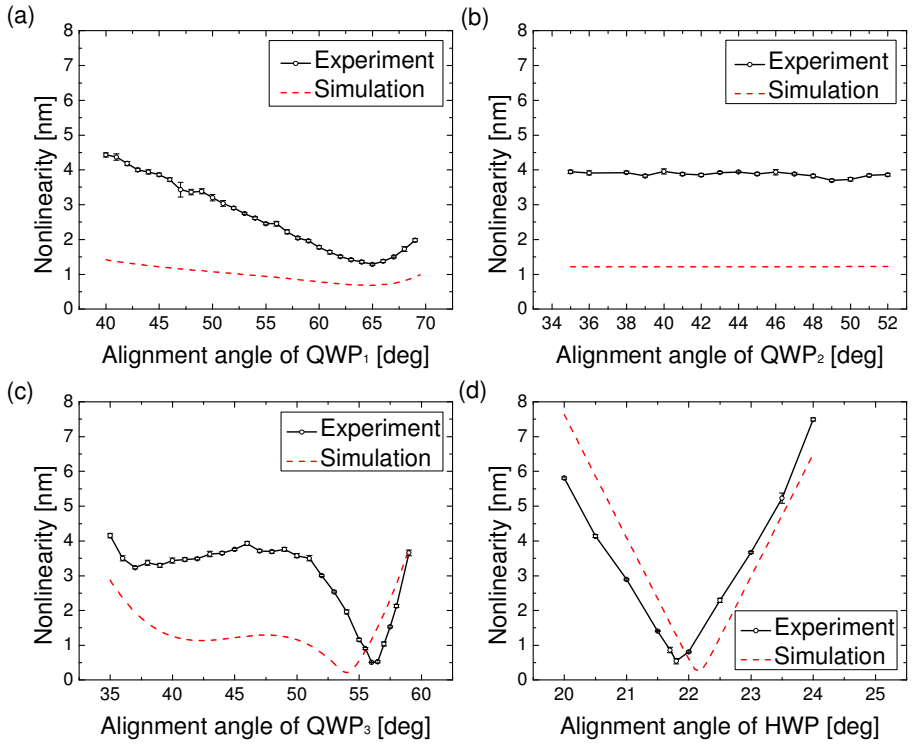

Fig. 6. Nonlinear error according to the alignment angle of wave plates: (a) QWP_1, (b) QWP_2, (c) QWP_3, (d) HWP

In the experiment, an iteration method is used to find the set of optimized alignment angles, because the theoretical expectation shows a little difference from the experiment result. The angular alignment of HWP and QWP_3 is highly sensitive, therefore, by adjusting them first near the expected angles, the optimized set can be easily obtained as 65.0° for QWP_1, 48.0° for QWP_2, 55.5° for QWP_3, and 21.3° for HWP. Finally, setting up WPs to this alignment angle set gives out 0.36 nm of nonlinearity as shown in Fig. 7, and only 0.12° of lack of quadrature is observed. Because, the lack of quadrature δ is almost removed as 0.12°, the main reason of remained nonlinearity is due to the electrical noise and short term power instability of laser.

Considering the difference between the theoretical and experimental results, more practical procedure is required when applying the proposed passive compensation method. Table 2 shows the steps for applying the passive compensation method practically when there is no theoretical approach. First step is to set up an interferometer with simple data processing. Next checking the nonlinearity variation is necessary for determining the specific alignment angles

#119009 - $15.00 USD Received 23 Oct 2009; revised 19 Nov 2009; accepted 19 Nov 2009; published 4 Dec 2009

of WPs. Some iteration method is required to find the optimized alignment angle set of WPs. Finally, the nonlinearity is minimized.

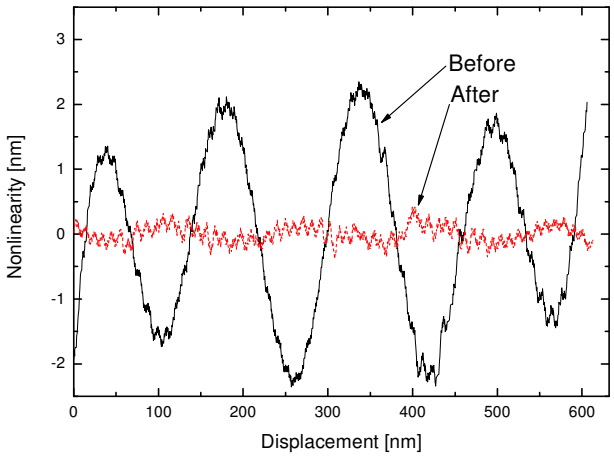

Fig. 7. Experimentally acquired nonlinearity: The passive compensation method suppresses the nonlinearity of the homodyne interferometer to one tenth in terms of the original peak-to-valley value.

Table 2. Step for applying the passive compensation method practically without theoretical approach.

Step 1: Setting up an interferometer
• Apply gain & offset correction to the raw signal of interferometer
↓
Step 2: Check the nonlinearity variation
• Rotate WPs ± 5° from the nominal value 45°, 22.5° • Check the direction which reduces the nonlinearity • Check the sensitivity of each WP for the nonlinearity
↓
Step 3: Adjust the alignment angle of WPs
• Rotate more sensitive WP in an orderly manner • Take an iteration method to find the optimized alignment angle set
↓
Step 4: Nonlinearity is removed

5. Conclusion

This study shows that the angular alignment of WPs should be adjusted according to the property of the PBS. As shown above, the passive compensation method suppressed the nonlinear error of homodyne interferometers to the sub-nanometer level, and it requires only simple calculation for processing the raw data. Therefore, it can be applied where sub-nanometer resolution and real-time compensation are required.

Acknowledgements

This work was supported by National Research Foundation of Korea through the Nano R&D Program (Grant 2009-0082848). Authors Jae Wan Kim and Soohyun Kim contributed equally to this paper.

#119009 - $15.00 USD Received 23 Oct 2009; revised 19 Nov 2009; accepted 19 Nov 2009; published 4 Dec 2009